

# High-efficiency WSi superconducting nanowire single-photon detectors for quantum state engineering in the near infrared

Hanna Le Jeannic,<sup>1,\*</sup> Varun B. Verma,<sup>2,\*</sup> Adrien Cavaillès,<sup>1</sup> Francesco Marsili,<sup>3</sup> Matthew D. Shaw,<sup>3</sup> Kun Huang,<sup>1</sup> Olivier Morin,<sup>4</sup> Sae Woo Nam,<sup>2</sup> and Julien Laurat<sup>1,†</sup>

<sup>1</sup>*Laboratoire Kastler Brossel, UPMC-Sorbonne Universités, CNRS,*

*ENS-PSL Research University, Collège de France, 4 Place Jussieu, 75005 Paris, France*

<sup>2</sup>*National Institute of Standards and Technology, 325 Broadway, Boulder, CO 80305, USA*

<sup>3</sup>*Jet Propulsion Laboratory, California Institute of Technology,*

*4800 Oak Grove Dr., Pasadena, California 91109, USA*

<sup>4</sup>*Max-Planck-Institut für Quantenoptik, Hans-Kopfermann-Str. 1, D-85748 Garching, Germany*

We report on high-efficiency superconducting nanowire single-photon detectors based on amorphous WSi and optimized at 1064 nm. At an operating temperature of 1.8 K, we demonstrated a 93% system detection efficiency at this wavelength with a dark noise of a few counts per second. Combined with cavity-enhanced spontaneous parametric down-conversion, this fiber-coupled detector enabled us to generate narrowband single photons with a heralding efficiency greater than 90% and a high spectral brightness of  $0.6 \times 10^4$  photons/(s·mW·MHz). Beyond single-photon generation at large rate, such high-efficiency detectors open the path to efficient multiple-photon heralding and complex quantum state engineering.

The near-infrared wavelength range has been an important playground for a large community in quantum optics, in particular at  $\lambda = 1064$  nm. At this wavelength that corresponds to Nd:YAG lasers, narrow-linewidth and ultra-stable lasers are available, as well as ultralow-loss optical coatings and photodiodes with close-to-unity efficiency. Pioneering [1] and world-record [2] demonstrations of squeezed light [3] have been performed at this wavelength, as well as quantum teleportation [4] and enhanced quantum metrology, including for gravitational wave detection [5]. In contrast to these realizations, the preparation of single-photon states or more complex states involving larger photon-number components generally requires single-photon detections to herald their preparations [6–8]. The efficient detection of single photons is therefore a fundamental and demanding requisite for these investigations [9]. This is particularly true for multiple heraldings, a challenging trend for developing novel quantum state engineering capabilities and further scalability in quantum networks [10].

However, detecting efficiently single photons at  $\lambda = 1064$  nm has been a long-standing issue. Avalanche photodiodes (APDs) based on Silicon are limited to a few percent quantum efficiency. InGaAs/InP ones, even though large improvements have been obtained in the recent years with these devices, still exhibit limited efficiency for this specific wavelength and often suffer from large dark count rates if used in free-running mode. In this wavelength range, the first generation of NbN superconducting nanowire single-photon detectors [11] (SNSPDs) were also limited to 20-30% efficiencies.

Recently, the development of SNSPDs based on tungsten silicide (WSi) [12, 13] enabled to outperform other

infrared single-photon detectors, despite great progresses with NbN-based devices [14, 15]. In addition to a better internal efficiency than other materials, the amorphous nature of WSi facilitates the fabrication of large sensitive area and the embedding of the material inside an optical stack to enhance absorption. System detection efficiency (SDE) greater than 90% has been achieved in the wavelength range  $\lambda = 1520 - 1610$  nm [16]. Efficient operation above 2 K has also been demonstrated at 1310 nm [17].

In this paper, we report on the optimization of WSi SNSPD at  $\lambda = 1064$  nm. A system detection efficiency of  $93 \pm 3\%$  is achieved with a dark noise below a few counts per second. As an application, we show the fast heralding of narrowband single photons. Based on a 53-MHz bandwidth optical parametric oscillator (OPO) with a close-to-unity escape efficiency, a heralding efficiency (i.e. the probability of finding a single photon in a given spatio-temporal mode per heralding event) greater than 90% and a heralding rate up to 1 MHz are demonstrated. The spectral brightness,  $\sim 0.6 \times 10^4$  photons/(s·mW·MHz), has been improved by more than 15 fold relative to our previous realizations and makes our system one of the brightest parametric-down conversion sources to date.

The  $W_{0.8}Si_{0.2}$  detectors, as shown in Fig. 1, were optimized for maximum absorption at 1064 nm. Simulations were performed via a Matlab program running RCWA (rigorously coupled-wave analysis) to optimize the layer thicknesses, given the optical constants of the materials (Fig. 1b). The first step of the fabrication process consists in the deposition of a 80 nm-thick gold mirror on a 3" Si wafer by electron beam evaporation and lift-off, with a 2 nm Ti adhesion layer below and above the mirror. A quarter-wave spacer layer (152 nm of SiO<sub>2</sub>) was then deposited by plasma-enhanced chemical vapor deposition, and Ti/Au contact pads were patterned by electron beam evaporation and lift-off. The  $\sim 4$  nm-thick superconductor layer was deposited by DC mag-

\* These authors contributed equally.

† julien.laurat@upmc.fr

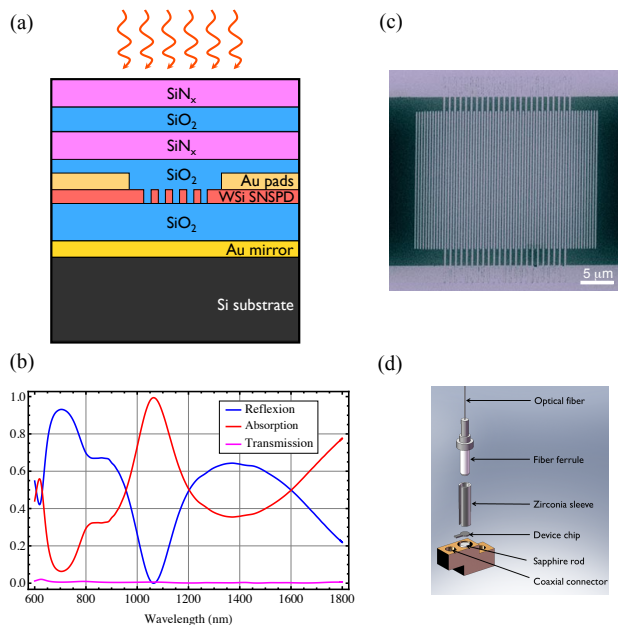


FIG. 1. (a) The WSi meander is embedded inside an optical stack deposited on a Si substrate. The layers have been optimized to enhance absorption at 1064 nm. An antireflection coating is deposited on the top surface and a quarter-wave spacer layer is realized between the meander and the bottom gold mirror. (b) Theoretical absorption, reflection and transmission spectra for the optimized layers. (c) SEM image of the meander. The nanowire has a width of 140 nm and pitch of 245 nm. (d) Detector assembly and fiber connection. The single-mode fiber is self-aligned via a zirconia sleeve. The  $16 \mu\text{m} \times 16 \mu\text{m}$  active area of the SNSPD is larger than the  $10 \mu\text{m}$  mode field diameter of a standard single-mode fiber, to allow for slight misalignment.

neutron cosputtering from separate W and Si targets at room temperature. It was then capped with 2 nm of amorphous Si to prevent oxidation. Photolithography and etching in an SF<sub>6</sub> plasma were used to define a  $20 \mu\text{m}$ -wide strip between gold contact pads. Electron beam lithography using PMMA resist and etching in SF<sub>6</sub> were then used to define nanowire meanders with a width of 140 nm and pitch of 245 nm within the  $20 \mu\text{m}$ -wide strip. An SEM image of the meander is shown on Fig. 1c. An antireflection coating was deposited on the surface with 102 nm SiO<sub>2</sub>, 137 nm SiN<sub>x</sub>, 171 nm SiO<sub>2</sub>, and 192 nm SiN<sub>x</sub>. Finally, a keyhole shape was etched through the wafer around each detector, which could then be removed and self-aligned to a single-mode fiber to within  $\pm 3 \mu\text{m}$  [18]. The keyhole part is attached on the top of a sapphire rod and bonded using aluminium microwires to a piece of copper in contact with an RF cable, as shown in Fig. 1d.

The SNSPD is mounted at the bottom of a double-wall dipstick, which is immersed in a liquid Helium dewar and pumped to achieve a 1.8 K operation temperature. A 1 meter-long single-mode optical fiber is connected to the detector and embedded inside the dipstick. The fiber

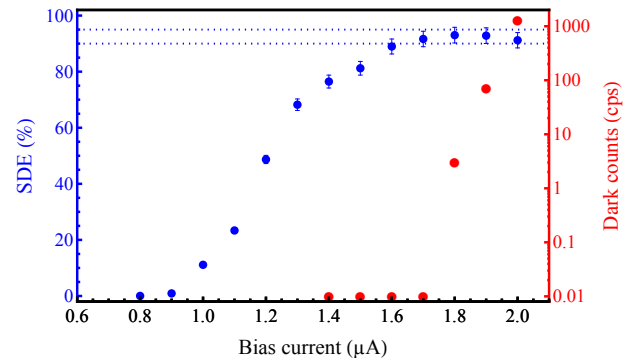


FIG. 2. System detection efficiency (SDE) at 1064 nm (blue) and dark counts (red) as a function of the bias current. For a bias current of  $1.8 \mu\text{A}$ , a value equal to 0.9 times the switching current, a SDE of  $93 \pm 3\%$  is obtained with a dark noise of 3 cps. These measurements are obtained at an operating temperature of 1.8 K.

end face is AR coated. Voltage pulses resulting from photon detection are first filtered by a 100 MHz low-pass filter then amplified via a chain of two 1 GHz amplifiers with 24 dB of gain each (Minicircuits ZFL-1000LN+), all operating at room temperature.

To quantify the overall system detection efficiency (SDE), which includes fiber and connexion losses, we use a strongly attenuated continuous-wave Nd:YAG laser with a mean photon-number of about 100,000 photons/s. As the detector is polarization sensitive (typically up to 10% difference in efficiency), the polarization of the probe light is optimized to maximize the number of counts. The main uncertainty is coming from the power-meter accuracy (Ophir PD300-IRG), i.e. 3%. The standard error on the count rate and the laser power fluctuations were measured to be below the percent level.

Figure 2 provides the measurement of the SDE and dark count rate as a function of the bias current. As it can be seen, at this operating temperature the system reaches the inflection current leading to a saturated efficiency before reaching the switching current,  $\sim 2 \mu\text{A}$ , for which the device switches to the normal non-superconducting state. At a bias current of  $1.8 \mu\text{A}$ , an SDE of  $93 \pm 3\%$  is obtained with a dark noise limited to 3 counts per second (cps). For bias currents closer to the switching current, the dark count rate increases rapidly.

We now turn to an application, namely the use of this optimized detector for heralding the generation of single photons. Preparing high-purity single photons at a large rate and into a well-controlled spatio-temporal mode is a crucial requirement for a variety of quantum information protocol implementations [19, 20]. We use here a general conditional preparation method based on twin beams [21–23] where the detection of one photon of the pair heralds the presence of the second one [24–36].

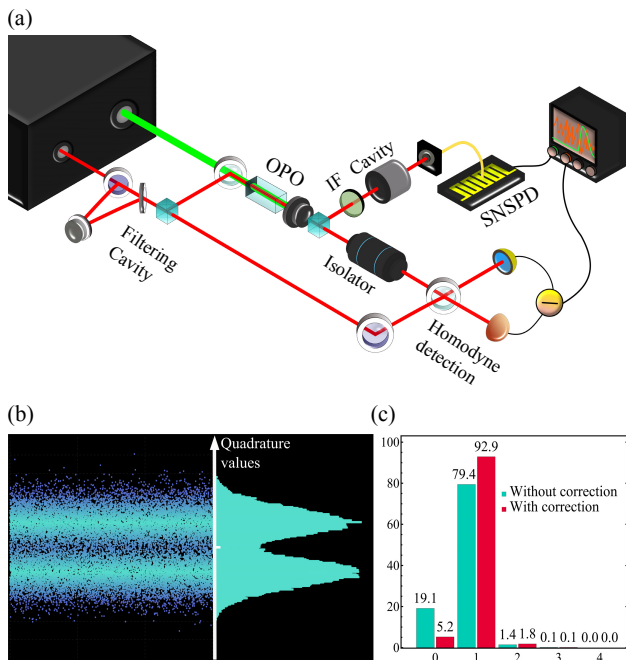


FIG. 3. (a) Experimental setup for the heralded single-photon source. A polarization non-degenerate and triply-resonant OPO is pumped far below threshold by a continuous-wave laser at 532 nm. Due to the cavity enhancement, the pump power is in the mW range. At the output of the OPO, photons pairs are separated via a polarizing beam splitter. Single-photon detection on the conditioning path heralds the emission of its twin, which is then characterized by homodyne detection. The overall transmission of the conditioning path, which includes frequency filtering (interferential filter IF and resonant cavity), reaches 50%. An optical isolator enables to avoid any backscattering from the detection system. (b) Quadrature values and distribution measured via the homodyne detection. (c) Photon-number distribution for a 1mW pump power, with and without correction from detection losses (15%). The heralding efficiency, i.e. the probability of obtaining a single photon per heralding event, reaches 93%. The vacuum admixture is limited to 5%.

The experimental setup is sketched in Figure 3a and has been described elsewhere [37–39]. It is based on a triply-resonant optical parametric oscillator made of a semi-monolithic linear cavity with on one side a 1cm-long coated KTP crystal ( $R = 95\%$  for 532 nm and HR for 1064 nm) and on the other side a curved output mirror (HR for 532 nm and  $R = 90\%$  for 1064 nm). This design provides a close-to-unity escape efficiency  $\eta_{OPO} = T/(T + L) = 0.96$  with  $T$  the transmission of the output coupler and  $L$  the residual intracavity losses. This parameter quantifies the intrinsic loss of the source and a value close to unity enables to obtain a very low admixture of vacuum, and therefore a large heralding efficiency. In complex state engineering, this low admixture enables to generate high-purity states with a large negativity of the associated Wigner function [7].

In our scheme, photon pairs emitted at 1064 nm with

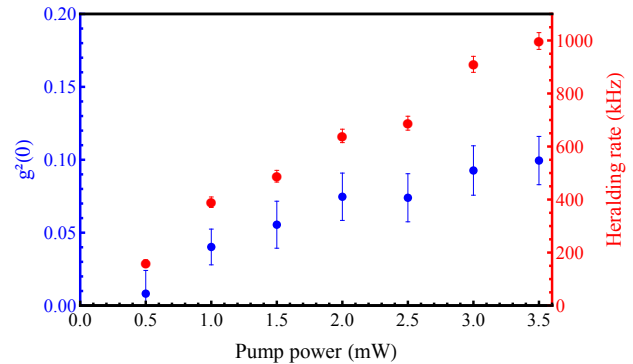


FIG. 4. Heralding rate and conditional autocorrelation function  $g^{(2)}(0)$  as a function of the pump power. A spectral brightness as large as  $0.6 \times 10^4$  photons/(s·mW·MHz) is obtained, close to the maximal achievable value in this parametric down-conversion system.

orthogonal polarizations are separated on a polarizing beam splitter. The idler photons are then frequency filtered by an interferential filter (0.5 nm bandwidth) and a Fabry-Perot cavity (300 MHz bandwidth), to select photons only in the central frequency mode of the OPO cavity. The overall transmission of the filtering path is measured to be  $\sim 50\%$ . These photons are finally detected by the WSi SNSPD and herald the generation of single photons on the signal mode. The heralded photons are then characterized using balanced homodyne detection. A few-mW laser beam (local oscillator, filtered by a high-finesse cavity) is mixed with the heralded state. Interference visibility above 99% is achieved. The two beam-splitter outputs are detected via two photodiodes and the photocurrents are then subtracted. This difference gives access to the quantum fluctuations of the signal that can be used to reconstruct the density matrix via a maximum-likelihood algorithm. Figure 3b shows the measured quadrature values and the associated distribution for a 1mW pump power. The temporal mode of the heralded state used here is a double-decaying exponential profile, as determined by the 53-MHz bandwidth of the OPO cavity [40].

Figure 3c provides the reconstructed diagonal elements of the density matrix, i.e. here the weight of the different photon-number components, including the vacuum component. The single-photon component reaches  $79 \pm 0.5\%$  without any correction from detection losses. By taking into account detection losses (limited to 15%), the single-photon weight is estimated to be  $93 \pm 0.5\%$ . This value corresponds to the heralding efficiency, i.e. the probability of finding a single photon in a given spatio-temporal mode per heralding event. The residual vacuum component is as low as  $5 \pm 0.5\%$ , a value consistent with the OPO escape efficiency.

Figure 4 finally provides the heralding rate and the

conditional autocorrelation function  $g^{(2)}(0)$  for the heralded state as a function of the continuous-wave pump power. The correlation function can be calculated from the measured photon-number components as  $g^{(2)}(0) = \frac{\langle (a^\dagger)^2 a^2 \rangle}{\langle a^\dagger a \rangle^2} \simeq \frac{2P_2}{(P_1 + 2P_2)^2}$  with  $P_1$  and  $P_2$  the single- and two-photon components. This parameter, which goes to zero for single-photon Fock state, increases with the unwanted multi-photon components. As a typical parametric down-conversion scheme, rate and  $g^{(2)}(0)$  have to be compromised. By increasing the pump power, we varied the heralding rate from 150 kHz to 1 MHz, with a  $g^{(2)}(0)$  ranging from 0.008 to 0.1.

The achieved spectral brightness is equal to  $0.6 \times 10^4$  photons/(s·mW·MHz). This value corresponds to a  $\sim 15$ -fold improvement relative to our previous works [37]. Notably, this value is close to the maximal achievable value in this parametric down-conversion system, namely  $\sim 1.2 \times 10^4$  photons/(s·mW·MHz) if one assumes perfect single-photon detector and no loss in the heralding path.

In conclusion, we reported the optimization of high-efficiency WSi superconducting nanowire single-photon detector at 1064 nm. At 1.8 K, the system detection efficiency reaches 93% with a background noise limited to a few counts per second. This efficiency is the highest demonstrated to date for this wavelength. Using this SNSPD to herald the generation of single photons, we

demonstrated a bright single-photon source that gathers a heralding efficiency larger than 90% and a narrowband spectrum. The unique combination of large escape efficiency OPOs, which enable a very low admixture of vacuum, and superconducting single-photon detectors with close-to-unity efficiency, as achieved here, will make protocols based on multiple-photon conditioning more accessible and scalable. It also opens the path to a variety of realizations in the developing optical hybrid approach to quantum information where discrete- and continuous-variables states, operations, and toolboxes are combined [41]. Our recent demonstration of high-rate generation of large squeezed optical Schrödinger cat states that relies on double heralding is a first example [8].

## ACKNOWLEDGMENTS

This work was supported by the European Research Council (Starting Grant HybridNet). Part of this research was carried out at the Jet Propulsion Laboratory, California Institute of Technology, under a contract with the National Aeronautics and Space Administration. V.B.V. and S.W.N. acknowledge partial funding for detector development from the DARPA Information in a Photon (InPho) and QUINNESS programs. J.L. is a member of the Institut Universitaire de France.

- 
- [1] L-A. Wu, H.J. Kimble, J.L. Hall, and H. Wu, Generation of squeezed states by parametric down conversion, *Phys. Rev. Lett.* **57**, 2520 (1986).
  - [2] T. Eberle *et al.*, Quantum enhancement of the zero-area Sagnac interferometer topology for gravitational wave detection, *Phys. Rev. Lett.* **104**, 251102 (2010).
  - [3] U. L. Andersen, T. Gehring, C. Marquardt and G. Leuchs, 30 years of squeezed light generation, *Phys. Scr.* **91**, 053001 (2016).
  - [4] W.P. Bowen *et al.*, Experimental investigation of continuous variable quantum teleportation, *Phys. Rev. A* **67**, 032302 (2003).
  - [5] J. Aasi *et al.*, Enhanced sensitivity of the LIGO gravitational wave detector by using squeezed states of light, *Nat. Photonics* **7**, 613 (2013).
  - [6] F. Dell'Anno, S. De Siena, and F. Illuminati, Multi-photon quantum optics and quantum state engineering, *Phys. Rep.* **428**, 53 (2006).
  - [7] O. Morin *et al.*, Remote creation of hybrid entanglement between particle-like and wave-like optical qubits, *Nat. Photonics* **8**, 570 (2014).
  - [8] K. Huang *et al.*, Optical synthesis of large-amplitude squeezed coherent-state superpositions with minimal resources, *Phys. Rev. Lett.* **115**, 023602 (2015).
  - [9] R.H. Hadfield, Single-photon detectors for optical quantum information applications, *Nat. Photonics* **3**, 696 (2009).
  - [10] I.A. Walmsley, Quantum optics: Science and technology in a new light, *Science* **348**, 525 (2015).
  - [11] C.M. Natarajan, M.G. Tammer, and R.H. Hadfield, Superconducting nanowire single-photon detectors: physics and applications, *Supercond. Sci. Technol.* **25**, 063001 (2012).
  - [12] B. Baek, A. Lita, V. Verma, and S.W. Nam, Superconducting a-W<sub>x</sub>Si<sub>1-x</sub> nanowire single-photon detector with saturated internal quantum efficiency from visible to 1850 nm, *Appl. Phys. Lett.* **98**, 251105 (2011).
  - [13] V.B. Verma *et al.*, A three-dimensional, polarization-insensitive superconducting nanowire avalanche photodetector, *Appl. Phys. Lett.* **101**, 251114 (2012).
  - [14] D. Rosenberg, A.J. Kerman, R.J. Molnar, and E.A. Dauler, High-speed and high-efficiency superconducting nanowire single photon detector array, *Opt. Express* **21**, 1440 (2013).
  - [15] S. Miki, T. Yamashita, H. Terai, and Z. Wang, High performance fiber-coupled NbTiN superconducting nanowire single photon detectors with Gifford-McMahon cryocooler, *Opt. Express* **21**, 10208 (2013).
  - [16] F. Marsili *et al.*, Detecting Single Infrared Photons with 93% System Efficiency, *Nature Photon.* **7**, 210 (2013).
  - [17] V.B. Verma *et al.*, High-efficiency WSi superconducting nanowire single-photon detectors operating at 2.5 K, *Appl. Phys. Lett.* **105**, 122601 (2014).
  - [18] A.J. Miller, A.E. Lita, B. Calkins, I. Vayshenker, S.M. Gruber, and S.W. Nam, Compact cryogenic self-aligning fiber-to-detector coupling with losses below one percent, *Opt. Express* **19**, 9102 (2011).
  - [19] M.D. Eisaman, J. Fan, A. Migdall, and S.V. Polyakov,

- Invited review article: single-photon sources and detectors, *Rev. Sci. Instrum.* **82**, 071101 (2011).
- [20] N. Gisin and R. Thew, Quantum communication, *Nature Photon.* **1**, 165 (2007).
- [21] C.K. Hong and L. Mandel, Experimental realization of a localized one-photon state, *Phys. Rev. Lett.* **56**, 58 (1986).
- [22] A.I. Lvovsky *et al.*, Quantum state reconstruction of the single-photon Fock state, *Phys. Rev. Lett.* **87**, 050402 (2001).
- [23] V. D'Auria, O. Morin, C. Fabre and J. Laurat, Effect of the heralding detector properties on the conditional generation of single-photon states, *Eur. Phys. J. D* **66**, 249 (2012).
- [24] J. S. Neergaard-Nielsen, B. Melholt Nielsen, H. Takahashi, A. I. Vistnes, and E. S. Polzik. High purity bright single photon source. *Optics Express*, Vol. **15**, 7940-7949 (2007).
- [25] P.J. Mosley, J.S. Lundeen, B.J. Smith, P. Wasylczyk, A.B. U'Ren, C. Silberhorn, and I. A. Walmsley, Heralded Generation of Ultrafast Single Photons in Pure Quantum States, *Phys. Rev. Lett.* **100**, 133601 (2008).
- [26] M. Scholz, L. Koch, and O. Benson, Statistics of narrow-band single photons for quantum memories generated by ultra bright cavity-enhanced parametric down-conversion, *Phys. Rev. Lett.* **102**, 063603 (2009)
- [27] F. Wolgramm, Y.A. de Icaza Astiz, F. Beduini, A. Cerè, and M. Mitchell, Atom-resonant heralded single-photons by interaction-free measurement, *Phys. Rev. Lett.* **106**, 053602 (2011).
- [28] S. Ramelow, A. Mech, M. Giustina, S. Groeblacher, W. Wieczorek, A. Lita, B. Calkins, T. Gerrits, S. W. Nam, A. Zeilinger, and R. Ursin, Highly efficient heralding of entangled single photons, *Opt. Express* **21**, 6707-6717 (2013).
- [29] E. Pomarico, B. Sanguinetti, T. Guerreiro, R. Thew, and H. Zbinden, MHz rate and efficient synchronous heralding of single photons at telecom wavelengths, *Optics Express* **20**, 23846 (2012).
- [30] S. Krapick, H. Herrmann, V. Quiring, B. Brecht, H. Suche, and C. Silberhorn, An Efficient Integrated Two-Color Source for Heralded Single Photons, *New Journal of Physics* **15** (2013), 033010.
- [31] J. Fekete, D. Rieländed, M. Cristiani, and H. de Riedmatten, Ultranarrow-band photon-pair source compatible with solid state quantum memories and telecommunication networks, *Phys. Rev. Lett.* **110**, 220502 (2013).
- [32] M. Förtsch, J.U. Fürst, C. Wittmann, D. Strekalov, A. Aiello, M.V. Chekhova, C. Silberhorn, G. Leuchs, and C. Marquardt, A versatile source of single photons for quantum information, *Nature Com.* **4**, 1818 (2013).
- [33] R.-B. Jin, M. Fujiwara, T. Yamashita, S. Miki, H. Terai, Z. Wang, K. Wakui, R. Shimizu, M. Sasaki, Efficient detection of a highly bright photon source using superconducting nanowire single photon detectors, *Optics Commun.* **336**, 47 (2015).
- [34] M. Fuwa, S. Takeda, M. Zwierz, H.M. Wiseman, and A. Furusawa, Experimental proof of nonlocal wavefunction collapse for a single particle using homodyne measurements, *Nat. Communications* **6**, 6665 (2015).
- [35] L. A. Ngah, O. Alibart, L. Labonté, V. D'Auria, and S. Tanzilli, Ultra-fast heralded single photon source based on telecom technology, *Laser and Photon. Rev.*, vol. **9**, L1-L5 (2015).
- [36] K.-H. Luo, H. Herrmann, S. Krapick, B. Brecht, R. Ricken, V. Quiring, H. Suche, W. Sohler, C. Silberhorn, Direct generation of genuine single-longitudinal-mode narrowband photon pairs, *New J. Phys.* **17**, 073039 (2015).
- [37] O. Morin, V. D'Auria, C. Fabre, and J. Laurat, High-fidelity single-photon source based on a Type II optical parametric oscillator, *Opt. Lett.* **37**, 3738 (2012).
- [38] O. Morin, J. Liu, K. Huang, F. Barbosa, C. Fabre, and J. Laurat, Quantum state engineering of light with continuous-wave optical parametric oscillators, *J. Vis. Exp.* **87**, e51224 (2014).
- [39] O. Morin *et al.*, Witnessing trustworthy single-photon entanglement with local homodyne measurements, *Phys. Rev. Lett.* **110**, 130401 (2013).
- [40] O. Morin, C. Fabre, and J. Laurat, Experimentally accessing the optimal temporal mode of traveling quantum light states, *Phys. Rev. Lett.* **111**, 213602 (2013).
- [41] U.L. Andersen, J.S. Neergaard-Nielsen, P. van Loock and A. Furusawa, Hybrid discrete- and continuous-variable quantum information, *Nature Phys.* **11**, 713 (2015).